Abundance and stratification analysis of the chemically peculiar star HD 103498

Chhavi P. Pandey,[1,2]⋆ Denis V. Shulyak,[3] Tanya Ryabchikova[4] and Oleg Kochukhov[5]

[1]*Aryabhatta Research Institute of Observational Sciences, Nainital 263129, India*
[2]*Department of Physics, Kumaun University, Nainital 263002, India*
[3]*Institute of Astrophysics, Georg-August-University, Friedrich-Hund-Platz 1, D-37077 Göttingen, Germany*
[4]*Institute of Astronomy, Russian Academy of Sciences, Pyatnitskaya 48, 119017 Moscow, Russia*
[5]*Department of Physics and Astronomy, Uppsala University, Box 516, 751 20 Uppsala, Sweden*

ABSTRACT

The slow rotation and the absence of strong mixing processes in the atmospheres of chemically peculiar stars develop the ideal conditions for the appearance of abundance anomalies through the mechanism of microscopic particle diffusion. This makes these objects look spectroscopically and photometrically different from their 'normal' analogues. As a result, it is often difficult to accurately determine the atmospheric parameters of these stars, and special methods are needed for a consistent analysis of their atmospheres. The main aim of the present paper is to analyse atmospheric abundance and stratification of chemical elements in the atmosphere of the chemically peculiar star HD 103498. We find that there are two model atmospheres, computed with individual and stratified abundances, that provide a reasonable fit to the observed spectroscopic and photometric indicators: $T_{\rm eff} = 9300$ K, $\log g = 3.5$ and $T_{\rm eff} = 9500$ K, $\log g = 3.6$. It is shown that Mg has a large abundance gradient in the star's atmosphere with accumulation of Mg ions in the uppermost atmospheric layers, whereas Si demonstrates the opposite behaviour with accumulation in deep layers. In addition, a detailed non-local thermodynamic equilibrium (non-LTE) analysis showed that none of the Mg transitions under consideration is a subject of noticeable non-LTE effects. By comparing the photometry observations after transforming them to physical units, we estimated the radius of HD 103498 to be between $R = (4.56 \pm 0.77)$ R$_\odot$ for $T_{\rm eff} = 9300$ K, $\log g = 3.5$, and $R = (4.39 \pm 0.75)$ R$_\odot$ for $T_{\rm eff} = 9500$ K, $\log g = 3.6$ models, respectively. We note that the lack of suitable observations in absolute units prevents us from uniquely determining the $T_{\rm eff}$ of the star at the current stage of analysis.

Key words: stars: atmospheres – stars: chemically peculiar – stars: fundamental parameters – stars: individual: HD 103498.

1 INTRODUCTION

As the name indicates, chemically peculiar (CP) stars are unusual in chemical composition in comparison to that of normal stars with similar fundamental parameters. This family of stars resides on the upper main sequence and they contribute about 15–20 per cent of early B- to late F-type stars. The speciality of this group is that they hold the strong abundance anomalies in their atmospheres such as the non-uniform horizontal and vertical distributions of chemical elements, and/or surface magnetic fields of different intensities. The type of peculiarity varies from star to star and it depends upon a number of factors such as stellar effective temperature, rotational velocity, the presence of magnetic field, membership in binary stel-

lar systems, etc. Microscopic chemical diffusion, arising from a competition between radiative levitation and gravitational settling, is believed to be the main process behind this phenomenon, as first discussed by Michaud (1970).

HD 103498 is a characteristic example of an evolved star belonging to the so-called CP group of spectral type A (Ap) with a strong overabundance of Si, Fe and Cr in its atmosphere as follows from the recent analysis undertaken by Joshi et al. (2010). The authors aimed at the pulsation analysis of the star's atmosphere and performed only classical homogeneous abundance analysis based on scaled-solar metallicity model atmosphere. Their analysis did not provide clear evidence as to whether HD 103498 belongs to roAp (rapidly oscillating Ap) stellar group. They also noted that the chemical properties and a high effective temperature of the star are distinguishable among the known roAp stars. According to the recent spectropolarimetric observations by Auriére et al. (2007), this

⋆ E-mail: chhavi.pandey@gmail.com

star has a weak longitudinal field $\langle B_z \rangle$ that varied between ± 200 G with a period of 15.83 d.

In this work we extend the study of Joshi et al. (2010) and carry out a complex, self-consistent analysis of the HD 103498 atmosphere. The main goal is to involve all the available observables to derive consistently the fundamental atmospheric parameters and abundance pattern of the star. We also look for the stratification of chemical elements and attempt to construct a self-consistent atmospheric model that fits the metallic line spectra, the hydrogen line profiles and the energy distribution of the star. This approach, where an iterative process is used for the derivation of atmospheric parameters, was already successfully applied in a number of recent investigations of normal (Ryabchikova, Fossati & Shulyak 2009) and peculiar (e.g. Kochukhov, Shulyak & Ryabchikova 2009; Shulyak et al. 2009, 2010) stars. The case of HD 103498 is of certain interest also because of its relatively high (as for roAp stars) temperature ($T_{eff} \approx 9500$ K) at which such important spectroscopic indicators as hydrogen lines become sensitive both to the atmospheric temperature and pressure stratification, making it difficult to separate the effects of T_{eff} and $\log g$. Thus other (photometric and/or spectrophotometric) observables must be simultaneously involved in the analysis to obtain precise results.

2 OBSERVATIONS

We used the average spectrum of HD 103498 which was obtained on 2009 February 2 (HJD 245 4865.624–245 4865.764) using the 2.56-m Nordic Optical Telescope (NOT) equipped with the Fibre-fed Echelle Spectrograph (FIES). The instrument was configured to use the high-resolution mode at the resolving power of $R = 47\,000$ in the spectral region $\lambda\lambda 3900$–7270. The FIES spectra were acquired at the magnetic phase range of 0.37 ± 0.2. The abundance analysis of the programme star is based on the average spectrum of time series spectroscopy. The finer details about the observations and data reduction procedure are given in Joshi et al. (2010).

We also made use of available photometric observations in Geneva (Rufener 1976), Johnson (Huchra & Willner 1973), Strömgren (Hauck & Mermilliod 1998), 2MASS (Skrutskie et al. 2006), and Δa (Paunzen, Stütz & Maitzen 2005) systems.

3 ANALYSIS TOOLS AND METHODOLOGY

3.1 Model atmospheres

To perform the model atmosphere calculations we used the recent version of the LLMODELS (Shulyak et al. 2004) stellar model atmosphere code. LLMODELS is a 1D, hydrostatic, plain-parallel local thermodynamic equilibrium (LTE) code that accounts for the effects of individual and stratified abundances. This program treats the bound–bound opacity by direct, line-by-line spectrum synthesis. The stratification of chemical elements is an input parameter for the code and thus is not changing during model atmosphere calculation process. This allows the exploration of the changes in the model structure due to the stratification that was extracted directly from the observations without modelling the processes that could be responsible for the observed inhomogeneities.

For every model atmosphere calculation the stellar atmosphere is discretized into 120 layers between $\log \tau_{5000} = -8$ and 2 with the higher point density in the region of steep abundance gradients to ensure an accurate integration of radiation field properties and solution of other equations. The frequency-dependent quantities are calculated with a variable wavelength step with a total of $\approx 520\,000$ wavelength points spread over the spectral region where the star radiates most of its energy. For the computation of line absorption coefficient, Vienna Atomic Line Database (VALD) data base (Piskunov et al. 1995; Kupka et al. 1999) was used as a source of atomic lines data.

3.2 Classical abundance analysis

The line identification in the observed spectrum of the star is based on the theoretical spectrum calculated for the entire observed spectral region using lines extracted from VALD. The spectrum synthesis code SYNTH3 (Kochukhov 2007) was used in all synthetic spectrum calculations. We compared synthetic and observed spectra to choose the least blended lines for the accurate abundance analysis using the IDL package BINMAG.[1]

The classical abundance analysis in the approximation of chemically homogeneous atmosphere is based on the analysis of equivalent widths of the lines, which is performed using the updated version (Tsymbal 1996) of the WIDTH9 code (Kurucz 1993). We adopted $\upsilon \sin i = 12$ km s^{-1} (obtained by the best fit to the observed unblended line profiles) and microturbulent velocity $\xi = 1.0 \pm 0.2$ km s^{-1} (derived from numerous lines of Cr I, Cr II, Fe I and Fe II) from Joshi et al. (2010). As the atmospheres of CP stars of type A are believed to be quiet in order to develop chemical peculiarities, a non-zero microturbulence found in (Joshi et al. 2010) probably results from the Zeeman broadening of spectral lines caused by a weak surface magnetic field. Since both in Joshi et al. and in the present study we use non-magnetic spectra synthesis, $\xi = 1.0$ km s^{-1} was still needed to mimic the effect of the star's magnetic field and its value were kept constant during iterative abundance analysis described below.

3.3 Stratified abundance analysis

To study the stratification of chemical elements in the atmosphere of the star we used the DDAFIT script which is an automatic procedure to find chemical abundance gradients from the observed spectra (Kochukhov 2007). DDAFIT provides an optimization and visualization interface to the spectrum synthesis calculations. In this routine, the vertical abundance distribution of an element is described with the four parameters: chemical abundance in the upper atmosphere, abundance in deep layers, the vertical position of abundance step and the width of the transition region where chemical abundance changes between the two values. All the four parameters can be modified simultaneously with the least-squares fitting procedure and are based on observations of an unlimited number of spectral regions. This procedure has been successfully applied in a number of studies (e.g. Ryabchikova et al. 2002; Ryabchikova, Leone & Kochukhov 2005; Ryabchikova et al. 2006; Kochukhov, Shulyak & Ryabchikova 2009; Shulyak et al. 2009, 2010).

3.4 Non-LTE analysis codes

To analyse the non-LTE effects on the Mg I/Mg II ions we used the DETAIL and SURFACE codes originally developed by Butler and Giddings (Giddings 1981; Butler 1984). Our calculations take into account the recent improvements in the atomic data for Mg. The extensive description of its model atom and non-LTE line formation are presented in Przybilla et al. (2001) and we refer the interested reader to the aforementioned paper.

---

[1] http://www.astro.uu.se/~oleg/

3.5 Self-consistent atmospheric modelling

Using the analysis techniques outlined above, it is possible to reconstruct the element distribution profile of any chemical species for which the accurate atomic data exist. However, it is to be noted that the empirical analysis of chemical elements' stratification depends upon the model atmosphere used, and the temperature–pressure structure of model atmosphere itself relies upon stratification. Consequently, the model atmosphere construction and stratified abundance analysis both are strongly coupled together. It is therefore necessary to use the iterative procedure which is described in the following steps.

(i) Selection of atmospheric parameters (first approximation, i.e. initially estimated parameters must be close to those of the star to be analysed; they can be either taken from the literature or estimated using available photometric calibrations).

(ii) Analysis of individual spectral lines to determine the stratification of chemical elements.

(iii) With the help of stratification found in the previous step, a new model must be calculated to provide an improved temperature–pressure structure of the stellar atmosphere.

(iv) Comparison of the modelled energy distribution (or/and photometric colours) and hydrogen line profiles with the observed ones. The model input parameters (T_{eff}, $\log g$) are then tuned to provide an agreement between theory and observations.

(v) Finally, the overall process from step 2 onwards must be repeated until stratification profiles of chemical elements and model parameters are converged.

The above-mentioned steps are schematically presented in Fig. 1. This procedure guarantees the consistency between the atmospheric model structure and abundances used for the calculation of synthetic line profiles.

The final self-consistent, chemically stratified model atmosphere is expected to reproduce simultaneously the observed photometry, energy distribution, hydrogen line profiles and metallic line spectra.
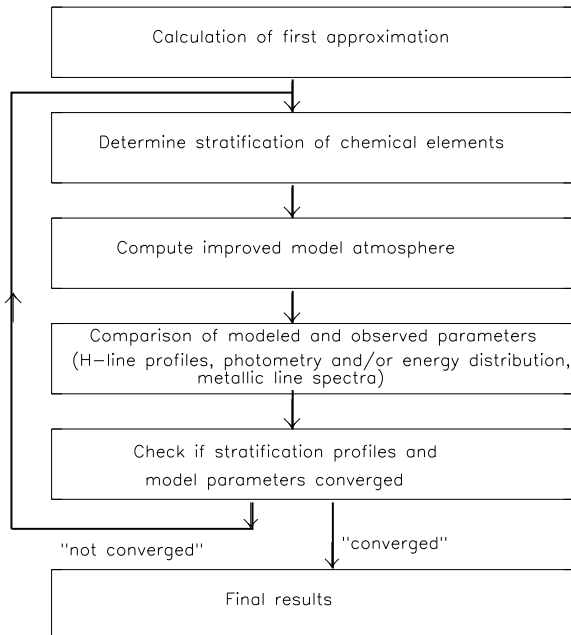

Figure 1. Steps used in the self-consistent models with an empirical abundance/stratification analysis.

Some recent examples of applying this procedure can be found in Kochukhov et al. (2009) and Shulyak et al. (2009, 2010).

4 RESULTS AND DISCUSSION

4.1 Fundamental atmospheric parameters

We used an iterative process in which the atmospheric parameters T_{eff}, $\log g$ and abundances are gradually improved by using different spectroscopic and photometric indicators. Using the calibration of Strömgren indices and Geneva photometry as implemented in the package TEMPLOGG^{TNG} (Kaiser 2006), as well as simultaneously fitting to the observed profiles of Hα and Hβ lines, Joshi et al. (2010) obtained the following atmospheric parameters: T_{eff} = 9500 K, $\log g$ = 3.6 employing the ATLAS9 (Kurucz 1992, 1993) model atmosphere computed with scaled solar abundances [M/H] = +0.5 dex. We used this model as the starting point in our analysis. Implementing the iterative procedure described in Section 3.5 two sets of parameters were obtained after five iterations as those providing, on an average, a good agreement between the observed and predicted spectroscopic and photometric observables: T_{eff} = 9300 K, $\log g$ = 3.5 and T_{eff} = 9500 K, $\log g$ = 3.6. As will be discussed later, in some cases hotter models provided a better fit to certain photometric parameters, but in those cases the ionization balance and the hydrogen lines were subjects of noticeable disagreements.

The results of abundance analysis show that the HD 103498 is a Cr–Fe rich star, and are consistent with those obtained before by Joshi et al. (2010). Table 1 summarizes the abundances obtained

Table 1. LTE homogeneous atmospheric abundances of HD 103498.

| Ion | This work | | | Joshi et al. | Sun |
	t9300g3.5	t9500g3.6	n	t9500g3.6	
C I	-4.20 ± 0.15	-4.11 ± 0.15	2	-4.11 ± 0.23	-3.65
O I	-3.81 ± 0.22	-3.79 ± 0.22	2	-3.92:	-3.38
Na I	-4.93 ± 0.16	-4.82 ± 0.20	2	-5.09:	-5.87
Mg I	-3.57 ± 0.14	-3.45 ± 0.14	5	-3.58 ± 0.13	-4.51
Mg II	-4.29 ± 0.35	-4.29 ± 0.35	5	-4.43 ± 0.27	-4.51
Al II	-6.21:	-6.25:	1	-6.06:	-5.67
Si I	-3.73 ± 0.32	-3.63 ± 0.32	4	-3.65 ± 0.33	-4.53
Si II	-3.94 ± 0.36	-3.99 ± 0.34	7	-3.64 ± 0.47	-4.53
Ca II	-5.87 ± 0.09	-5.79 ± 0.09	2	-5.91	-5.73
Ti II	-6.46 ± 0.17	-6.35 ± 0.17	25	-6.45 ± 0.16	-7.14
V II	-8.17 ± 0.18	-8.07 ± 0.18	2	-8.14 ± 0.18	-8.04
Cr I	-3.31 ± 0.18	-3.19 ± 0.19	101	-3.25 ± 0.23	-6.40
Cr II	-3.36 ± 0.22	-3.32 ± 0.22	230	-3.31 ± 0.24	-6.40
Mn I	-5.93 ± 0.10	-5.79 ± 0.10	2	-5.94 ± 0.11	-6.65
Mn II	-5.76 ± 0.24	-5.71 ± 0.24	3	-5.72 ± 0.23	-6.65
Fe I	-3.04 ± 0.16	-2.92 ± 0.16	105	-2.98 ± 0.20	-4.59
Fe II	-3.12 ± 0.18	-3.11 ± 0.18	169	-3.01 ± 0.18	-4.59
Co II	-5.62:	-5.57:	1	-5.58:	-7.12
Ni I	-5.33:	-5.21:	1	-5.34:	-5.81
Ba II	-8.72 ± 0.25	-8.53 ± 0.25	4	-8.64:	-9.87
Ce II	-9.16:	-8.96:	1	-9.10:	-10.46
Pr III	-9.02 ± 0.22	-8.91 ± 0.22	5	-8.87 ± 0.33	-11.33
Nd III	-8.51 ± 0.16	-8.40 ± 0.17	12	-8.41 ± 0.16	-10.59
Sm II	-8.76:	-8.58:	1	-8.70:	-11.03
Eu II	-8.94 ± 0.14	-8.72 ± 0.15	2	-8.85 ± 0.12	-11.53
Gd II	-8.63 ± 0.19	-8.47 ± 0.21	2	-8.72:	-10.92

Error estimates are based on the internal scattering from the number of the analysed lines, n. Abundances are given in $\log(N/N_{total})$. The last column gives the abundances of the solar atmosphere (Asplund, Grevesse & Sauval 2005).
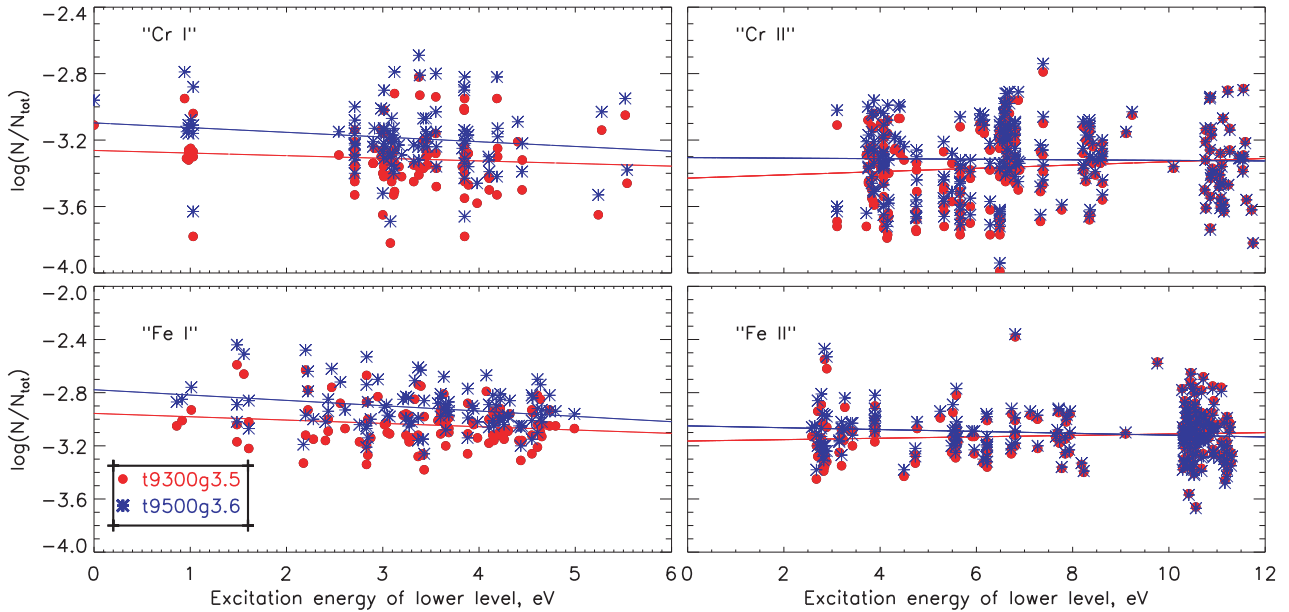
Figure 2. Plots of individual abundances for Cr I/Cr II(top) and Fe I/Fe II(bottom) lines as a function of excitation energy of the lower level for HD 103498 with two different models: red filled circles – $T_{\mathrm{eff}} = 9300$ K, $\log g = 3.5$; blue stars – $T_{\mathrm{eff}} = 9500$ K, $\log g = 3.6$.

using two model atmospheres. The differences between the abundances from Joshi et al. (2010) and ours for the $T_{\mathrm{eff}} = 9500$ K, $\log g = 3.6$ model are likely due to the changes in the atmospheric structure between the solar-scaled abundance model and the model atmosphere computed with the realistic chemistry of the star. In addition, the number of lines used for the abundance analysis is different between the two studies, which may also influence the final results. Nevertheless, the agreement is very good within the estimated error bars. As expected, the model with a cooler temperature statistically results on lower abundances as the computed atomic lines become stronger with the decrease in T_{eff} in this particular temperature regime.

Fig. 2 illustrates the ionization balance in the atmosphere of HD 103498 as derived using lines of Fe I/Fe II and Cr I/Cr II. There is not much difference between the two models, and the slopes are nearly the same, though the model with $T_{\mathrm{eff}} = 9500$ K provides a slightly better fit for the first ions, while the neutrals seem to prefer $T_{\mathrm{eff}} = 9300$ K.

4.2 Stratification of Si and Mg

Although HD 103498 is a Cr–Fe rich star, these two elements do not demonstrate any signature of a possible stratification. The abundances obtained from strong and weak lines of Fe and Cr were found to be nearly the same without noticeable patterns. Since lines with different excitation energies statistically probe different atmospheric layers, the absence of peculiar abundance patterns among strong and weak lines clearly shows the absence of strong abundance gradients in the stellar atmosphere, observed in the cooler CP stars (see, for example, fig. 3 in Ryabchikova 2008). Nevertheless, we checked the possible stratification with the DDAFIT package. We selected 17 lines of the neutral and singly ionized element for Cr and the same amount for Fe. The range of excitation energies were (0–3.45 eV) for Cr I lines, (3.71–11.10 eV) for Cr II lines, (0.86–3.39 eV) for Fe I lines, and (2.90–10.68 eV) for Fe II lines. The observed intensity varied from 11 to 300 mÅ. Formally, for both the elements we get a solution with a small steep abun-

dance gradient at $\log \tau_{5000} \approx -1$ which does not exceed 0.5 dex; however, a difference between standard deviation for homogeneous and stratified abundance distributions is insignificant. For both the elements, Cr and Fe, we get a small increase in the abundance towards the upper atmosphere (except Cr for $T_{\mathrm{eff}} = 9300$ K, $\log g = 3.5$). Similar distributions are observed in other CP stars of the same temperature range. The Cr abundance gradient is very small in HD 133792 with $T_{\mathrm{eff}} = 9400$ K (Kochukhov et al. 2006) and practically absent in HD 204411 with $T_{\mathrm{eff}} = 8700$ K (Ryabchikova et al. 2005). Recent diffusion calculations (LeBlanc et al. 2009; Alecian & Stift 2010) show that rather strong Cr and Fe abundance gradients with an accumulation in deeper atmospheric layers should be observed in the atmosphere of a star with $T_{\mathrm{eff}} = 9300$–9500 K having a small magnetic field, and these gradients disappear at much higher temperatures. A strong horizontal magnetic field influences the diffusion process resulting in an upward abundance gradient after an abundance minimum at $\log \tau_{5000} \approx -1$. In this case the step-function approximation is not valid anymore, and its employment leads to smearing the possible gradients. However, no indications exist in favour of the strong horizontal (toroidal?) component of magnetic field in HD 103498 as well as in HD 133792 and HD 204411.

A detailed inspection of the spectra of HD 103498 showed that only two elements are suitable for stratification analysis: Mg and Si. Both are represented by a sufficient number of strong and weak lines which are not blended much by nearby lines of others elements. These lines and their current parameters extracted from VALD are presented in Table 2.

Using the DDAFIT package we derived the stratification profiles of Mg and Si for the two selected model atmospheres. Fig. 3 demonstrates a run of abundances as a function of the atmospheric depth, and Fig. 4 illustrates the resulting best fit to individual line profiles. We find magnesium to be strongly overabundant in the upper atmosphere of HD 103498 and underabundant in deep layers. The abundance jump is very smooth, occupying a considerable region of atmospheric depths. It is noteworthy that in case all the four parameters of the assumed step-like abundance distribution were

Table 2. A list of spectral lines used for the stratification analysis.

Ion	Wavelength	E_i (eV)	$\log(gf)$	$\log\gamma_{\text{Stark}}$	Ref.
Mg II	4384.637	9.996	−0.790	−4.07	KP
Mg II	4390.514	9.999	−1.490	−4.07	KP
Mg II	4390.572	9.999	−0.530	−4.07	KP
Mg II	4433.988	9.999	−0.910	−4.40	KP
Mg II	4481.126	8.864	0.740	appx	KP
Mg II	4481.150	8.864	−0.560	appx	KP
Mg II	4481.325	8.864	0.590	appx	KP
Mg I	4702.991	4.346	−0.666	−3.98	LZ
Mg II	4739.593	11.569	−1.960	appx	KP
Mg II	4739.593	11.569	−0.660	appx	KP
Mg II	4739.709	11.569	−0.820	appx	KP
Mg I	5172.684	2.712	−0.402	appx	AZ
Mg I	5183.604	2.717	−0.180	appx	AZ
Mg I	5528.405	4.346	−0.620	−4.46	LZ
Mg I	5711.088	4.346	−1.833	appx	LZ
Si II	4130.872	9.839	−0.824	−4.87	BBCB
Si II	4190.707	13.492	−0.17	−5.26	MERL
Si II	5055.984	10.074	0.593	−4.78	SG
Si II	5056.317	10.074	−0.359	−4.78	SG
*Si II	5669.563	14.200	0.28	−5.53	BBC
*Si II	5688.817	14.186	0.13	−5.50	BBC
*Si II	5868.444	14.528	0.400	−5.36	MERL
Si II	5957.559	10.067	−0.301	−4.84	SG
Si I	6155.134	5.619	−0.754	−3.16	K07
Si II	6347.109	8.121	0.297	−5.04	BBCB

The columns give the ion identification, central wavelength, the excitation potential (in eV) of the lower level, oscillator strength [$\log(gf)$], the Stark damping constant ('appx' marks lines for which the classical approximation was used), and the reference for oscillator strength.
AZ, Anderson, Zilitis & Sorokina (1967); BBC, Blanco, Botho & Campos (1995); BBCB, Berry et al. (1971); LZ, Lincke & Ziegenbein (1971); KP, Kurucz & Peytremann (1975); K07, http://kurucz.harvard.edu/atoms/1400/; MERL, Matheron et al. (2001); SG, Smith & Gallagher (1966). Stark damping constants are taken from VALD except those marked by asterisk, which are taken from Wilke (2003).

minimized simultaneously (see Section 3.3 for explanations), the solution was always with big error bars for the value of the abundance in deep layers. We thus also tried to derive a stratification profile when abundances in these layers were fixed at constant values, from $\log(N/N_{\text{total}}) = -20$ dex to $\log(N/N_{\text{total}}) = -10$ dex (some examples are presented in Fig. 3). However, in all the cases the fit to Mg lines did not change much and the common feature of a strong abundance gradient between the surface and photospheric layers still stay. It is important to stress here that the values of abundances below $\log\tau_{5000} \approx 0$ have no strict physical meaning since these atmospheric layers are not visible to us and thus cannot be modelled by comparing observed and predicted line profiles. In other words, changing the abundances in these layers has no effect on the computed line profiles and hence the true abundances cannot be recovered in principle.

In addition we find that none of the Mg lines used for stratification analysis is a subject of strong deviations from the LTE, a fact that could affect the final results. Since the DETAIL/SURFACE package can only deal with homogeneous abundances, we used the original model atmosphere from Joshi et al. (2010) in order to estimate respective non-LTE abundance corrections $\Delta\log\epsilon = \log\epsilon_{\text{NLTE}} - \log\epsilon_{\text{LTE}}$, which are presented in Table 3. The largest non-LTE abundance correction was found for the Mg II 4481.126 Å line and is −0.05 dex.
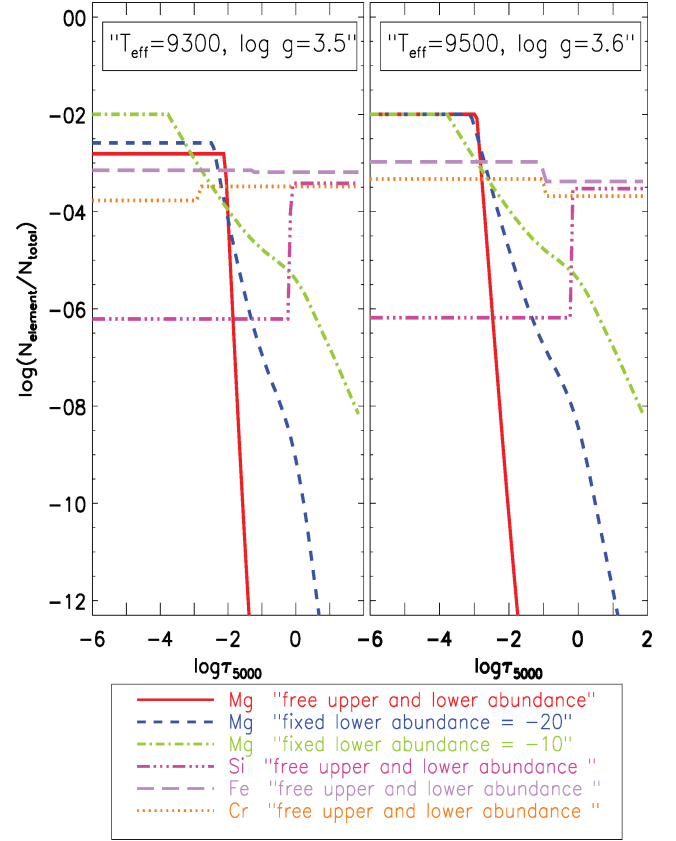

Figure 3. Stratification of Mg and Si in the atmosphere of HD 103498 derived using two models with $T_{\text{eff}} = 9300$ K (left-hand panel) and $T_{\text{eff}} = 9500$ K (right-hand panel) and different optimization settings for the step-like stratification profile. Full red line – optimization of all four parameters of the stratification profile of Mg; dashed blue line – lower abundance is fixed for Mg at $\log(N/N_{\text{total}}) = -20$ dex; dash–dotted green line – lower abundance is fixed for Mg at $\log(N/N_{\text{total}}) = -10$ dex; dash–three dots magenta line – optimization of all the four parameters of the stratification profile of Si; purple long-dashes – optimization of all the four parameters of the stratification profile of Fe; and finally dotted orange line – optimization of all four parameters of the stratification profile of Cr.

The stratification profile of Si was found to be similar to those frequently found in cooler CP stars, i.e. with accumulation in photospheric layers. Its shape did not change much between $T_{\text{eff}} = 9300$ and 9500 K models; only the abundance jump became steeper for the cooler one.

The fact that Mg stratification is opposite to that of Si, i.e. that Mg is pushed up by radiation much more effectively, is of course a very important result for the modern models of particle diffusion in stellar atmospheres, and the same behaviour of Mg was already found in another peculiar star, HD 204411 (see fig. 7 in Ryabchikova et al. 2005).

The obtained Mg distribution again can be explained qualitatively by diffusion in the presence of a very strong horizontal magnetic field (see fig. 3 in Alecian & Stift 2007). In principle, Si gradients are also predicted by diffusion models; however, neither Alecian & Stift (2007, 2010) nor LeBlanc et al. (2009) predict a strong Si overabundance at the photospheric layers, that is commonly observed in all stars investigated up to now. In all diffusion calculations the maximum of Si abundance is solar or slightly below the solar value.

The formal distributions of Fe and Cr are also shown in Fig. 3, but because of the relatively small abundance jumps (≤ 0.5 dex)
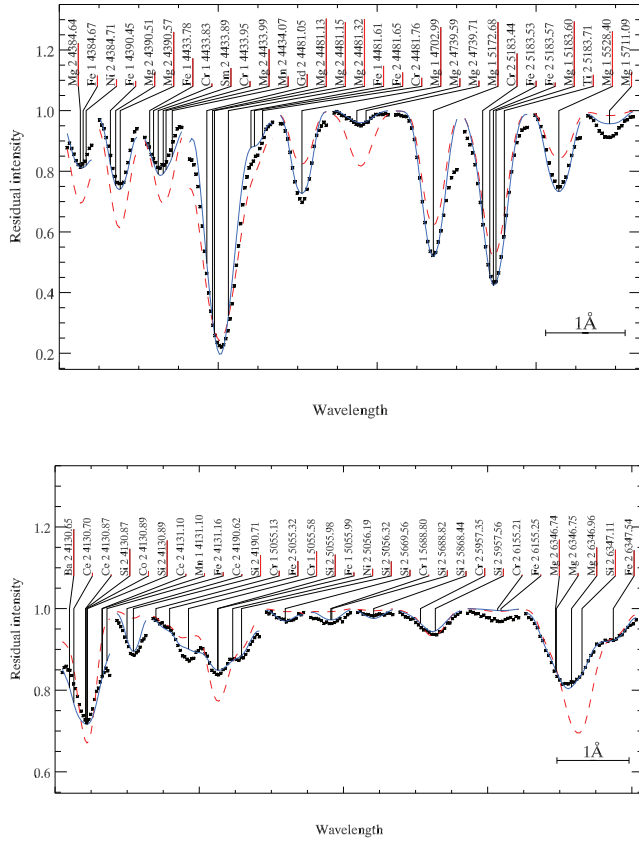
Figure 4. A comparison between the observed and predicted profiles of Mg (top panel) and Si (bottom panel). Dotted black line – observations; dashed red line – synthetic spectra computed with homogeneous abundances [$\log(N_{Mg}/N_{total}) = -3.87$, $\log(N_{Si}/N_{total}) = -4.95$] (in case of Si for initial guess we used the homogeneous abundance that gives the best fit to line profiles used for stratification analysis); solid blue line – synthetic spectra computed with the final stratified abundance distributions shown by solid red lines in Fig. 3.

Table 3. Non-LTE abundance corrections associated with each Mg I and Mg II transition used for stratification analysis. Columns 3 and 6 represent NLTE corrections for the star Vega (Przybilla et al. 2001).

| | $\Delta \log \epsilon$ | | | $\Delta \log \epsilon$ | |
Mg I	(HD 103498)	(Vega)	Mg II	(HD 103498)	(Vega)
4702.991	+0.01	+0.02	4384.637	−0.00	...
5172.684	−0.03	−0.06	4390.572	−0.00	+0.00
5183.604	−0.04	−0.13	4433.988	−0.00	+0.00
5528.405	−0.00	−0.03	4481.126	−0.05	−0.21
5711.088	+0.01	...	4739.593	+ 0.00	...

their distributions can be safely described as uniform (within the errors of standard deviations between the observed and predicted line profiles). Therefore, even if present, such weak abundance gradients of Fe and Cr would in no way affect the photometric and spectroscopic observables compared to the models computed with the simple homogeneous distributions assumed in the present work.

4.3 Energy distribution and hydrogen line profiles

Unfortunately, the lack of observed spectrophotometric or low-resolution spectroscopic energy distributions for HD 103498 did
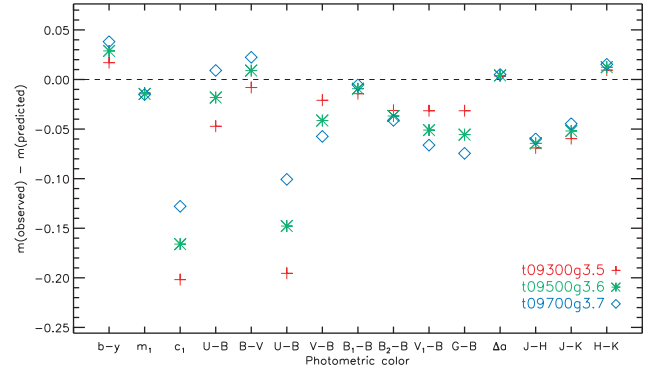

Figure 5. Difference between observed and predicted colours of different photometric systems. Theoretical colours were reddened applying $E(B - V) = 0.06$.

not allow us to uniquely derive its effective temperature. We therefore only attempted to use the available photometric observations in different systems. Fig. 5 illustrates the difference between the observed and computed photometric parameters for the three atmospheric models. All the photometric parameters were calculated using the modified computer codes given by Kurucz (1993), which take into account the transmission curves of individual photometric filters, mirror reflectivity and a photomultiplier response function. From the HIPPARCOS parallax of $\pi = 3.37 \pm 0.56$ mas (van Leeuwen 2007), the distance to the star is $d = 297$ pc, which results in a redenning value of $E(B - V) = 0.06$ by applying the extinction maps published by Amôres & Lépine (2005). In general, the two final models with $T_{eff} = 9300$ and 9500 K are in a reasonable agreement with observations except Strömgren c_1 and Geneva $U - B$ for which we find the largest deviation to be about 0.2 mag. As c_1 measures the amplitude of the Balmer jump, one would suppose that the true temperature or gravity of the star should be much higher than adopted in the present study. Indeed, increasing T_{eff} up to 9700 K improves the fit to c_1 significantly. However, in this case the fit to hydrogen lines becomes much worse. Last but not the least, the temperature-sensitive index $b - y$ clearly requires lower temperatures. The same concerns the gravity of the star: increasing $\log g$ also helps to get closer to the observed value of c_1, but then we find a disagreement between the observed and the predicted hydrogen lines as well as in the ionization balance between Fe I/Fe II and Cr I/Cr II.

To better understand the problem, we plotted the observed photometric parameters transformed to absolute fluxes and compared them with model predictions in Fig. 6. To obtained fluxes in physical units, we used calibrations by Rufener & Nicolet (1988) for the Geneva, by van der Bliek, Manfroid & Bouchet (1996) for the 2MASS, and by Bessell, Castelli & Plez (1998) for the Johnson photometry. As expected, infrared fluxes are not much sensitive to the temperature and gravity of models, but the strong deviation in Johnson and Geneva ultraviolet U indices is clearly visible.

The fit to the Balmer Hα and Hβ lines is presented on Fig. 7. Accounting for the stratification clearly helps to improve the fit to the observed line profiles compared to the spectra computed with only homogeneous abundances, but both spectra fail to fit the transition region between the cores and wings of the lines where theoretical profiles are systematically too much wide. The same holds true for the cooler model with $T_{eff} = 9300$ K (not shown in the figure for a better view). Still, the solar-scaled abundance model used by Joshi et al. (2010) seems to provide the best fit among all the models considered in this study; however, one should
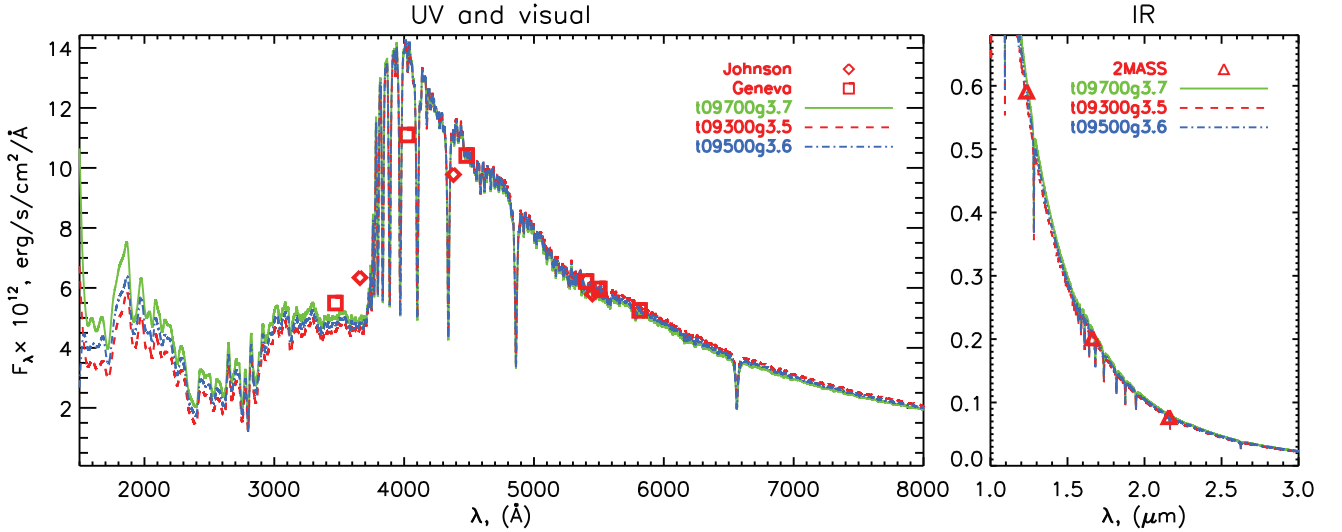
Figure 6. Comparison between the observed photometric parameters calibrated in absolute units and the theoretical fluxes convolved with FWHM = 5 Å Gaussian. Theoretical fluxes were reddened applying $E(B - V) = 0.06$.
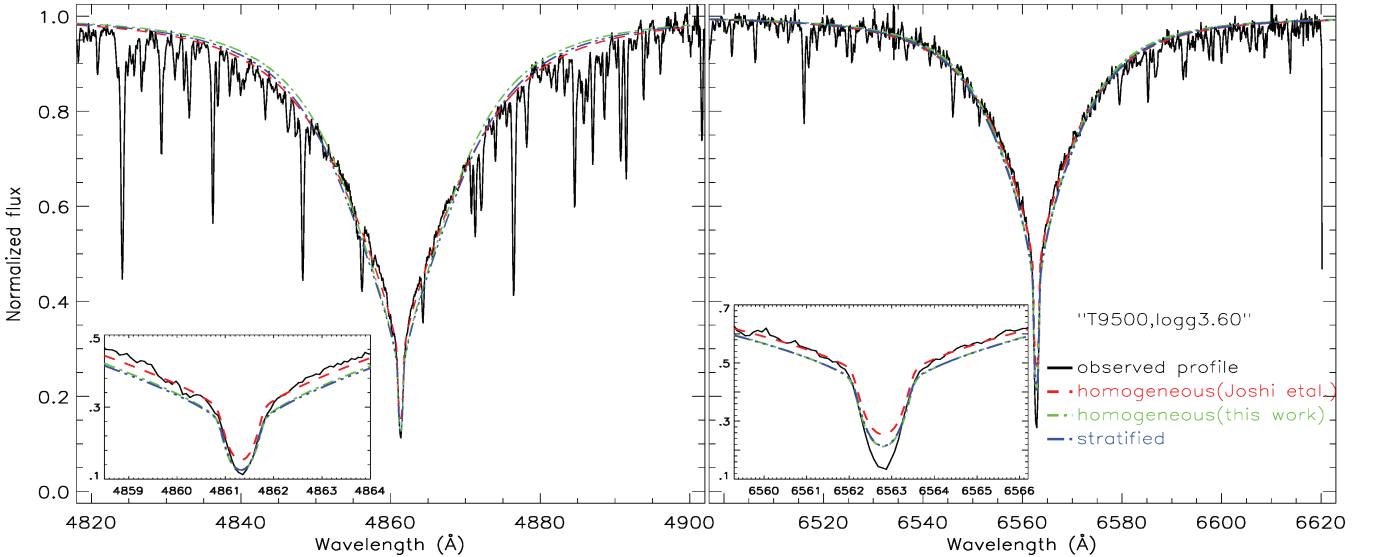

Figure 7. Comparison between the observed Hβ (left-hand panel), observed Hα (right-hand panel) and synthetic line profiles. Solid black line – observed profile; dashed red line – synthetic spectra computed with homogeneous abundances (Joshi et al. 2010); dash–dotted green line – synthetic spectra computed with homogeneous abundances (this work); dash–three dots blue line – synthetic spectra computed with stratified abundances. In both cases the final adopted model corresponds to $T_{\rm eff} = 9500$ K, $\log g = 3.6$. The inset shows the zoomed part of the profiles around the core of line.

not forget that this model is inconsistent with the true abundance pattern of the star: Joshi et al. (2010) used the ATLAS9 model with metallicity [M/H] = +0.5 dex, but the true iron overabundance of the star is ≈+1.5 dex compared to the Sun. Obviously, using now the respective homogeneous model with [M/H] = +1.5 dex would immediately result in wider profiles of hydrogen lines (due to an increase in the number of free electrons and thus Stark broadening), no longer providing a fit to line profiles.

From the analysis presented above it is clear that there is a fundamental disagreement between the temperatures of the star suggested by some photometric indicators and the hydrogen line profiles. The fitting energy distribution requires a temperature that is systematically higher than those followed from fitting the Hα and Hβ lines. We thus speculate that there could be few reasons for this, which

should be checked in future investigations. First of all, except Mg and Si other elements can be stratified in the atmosphere of HD 103498. If so and (as usually found) the stratification profiles are similar to that of Si, then the concentrations of free electrons in the upper atmospheric layers could become smaller than the one in the present study, thus resulting in narrower profiles of hydrogen lines. Unfortunately, as stated above, no good sets of lines for an accurate stratification analysis could be found for elements other than Mg and Si in the spectra of HD 103498. Also, the normalization of hydrogen lines in the echelle spectra is a complicated task and some systematic uncertainties may still influence fitting results.

Finally, a comparison of the observed photometry calibrated in absolute units and model fluxes allowed us to estimate the radius of

the star. With parallax $\pi = 3.37 \pm 0.56$ mas we obtained $R = (4.56 \pm 0.77)$ R$_\odot$ for $T_{\rm eff} = 9300$ K, $\log g = 3.5$ model and $R = (4.39 \pm 0.75)$ R$_\odot$ for $T_{\rm eff} = 9500$ K, $\log g = 3.6$ model, respectively.

5 CONCLUSIONS

In this work we carried out a detailed atmospheric abundance and stratification analysis of the chemically peculiar A0 star HD 103498, which is an extension of the analysis presented in Joshi et al. (2010). Using the available spectroscopic and photometric parameters, as well as the up-to-date model atmosphere and spectra synthesis codes, we attempted to construct a self-consistent model atmosphere of the star and to determine the fundamental atmospheric parameters iteratively by comparing various observables with the model predictions. Our main results are summarized in the following.

(i) We find that, generally, two model atmospheres computed with individual and stratified abundances provide a reasonable fit simultaneously to the spectroscopic and photometric indicators: $T_{\rm eff} = 9300$ K, $\log g = 3.5$ and $T_{\rm eff} = 9500$ K, $\log g = 3.6$. The latter model has the same parameters as the one used in Joshi et al. (2010), but, in contrast, includes the realistic chemistry of the star.

(ii) The abundance analysis demonstrates a strong overabundance of Fe and Cr relative to the Sun, and our results are in an excellent agreement with Joshi et al. (2010).

(iii) Using a simplified step-function approximation of the stratification profile, we derived depth-dependent distributions of Mg and Si. We show that Mg has a large abundance gradient in the atmosphere of HD 103498, with an accumulation of Mg ions in the uppermost atmospheric layers. The distribution of Si demonstrates the opposite behaviour with accumulation of Si ions in the deep atmospheric layers. This indicates that Mg is pushed up by radiative forces much more efficiently than Si. These empirical findings are certainly of interest for the modern theory of particle diffusion in stellar atmospheres.

(iv) Although the star is Cr–Fe rich, these two elements do not show any signature of noticeable stratification in its atmosphere.

(v) We find that none of the Mg transitions used for the stratification analysis is a subject of noticeable non-LTE effects. The largest non-LTE abundance correction was found for the Mg II 4481.126 Å line and is -0.05 dex.

(vi) Comparing the observed photometry in Strömgren, Geneva, 2MASS, and Johnson filters transformed to physical units with model fluxes, we estimated the radius of HD 103498 to be $R = 4.56 \pm 0.77$ R$_\odot$ for the $T_{\rm eff} = 9300$ K, $\log g = 3.5$ model and $R = 4.39 \pm 0.75$ R$_\odot$ for the $T_{\rm eff} = 9500$ K, $\log g = 3.6$ model, respectively.

(vii) A comparison of the observed photometric parameters and hydrogen line profiles for different model atmospheres showed that such indices as c_1 and $U - B$ systematically require hotter models and Hα, Hβ and $b - y$ index cooler models relative to the initially assumed temperature $T_{\rm eff} = 9500$ K. Unfortunately, the lack of suitable spectrophotometric or low-resolution spectroscopic observations in absolute units prevents us from uniquely determining the $T_{\rm eff}$ of the star.

REFERENCES

Alecian G., Stift M., 2007, A&A, 475, 659
Alecian G., Stift M., 2010, A&A, 516, A53
Amôres E. B., Lépine J. R. D., 2005, AJ, 130, 659
Anderson E. M., Zilitis V. A., Sorokina E. S., 1967, Opt. Spectrosc., 23, 102
Asplund M., Grevesse N., Sauval A. J., 2005, in Barnes T. G., III, Bash F. N., eds, ASP Conf. Ser. Vol. 336, Cosmic Abundances as Records of Stellar Evolution and Nucleosynthesis. Astron. Soc. Pac., San Francisco, p. 25
Auriére M. et al., 2007, A&A, 475, 1053
Berry H. G., Bromander J., Curtis L. J., Buchta R., 1971, Phys. Scr., 3, 125
Bessell M. S., Castelli F., Plez B., 1998, A&A, 333, 231
Blanco F., Botho B., Campos J., 1995, Phys. Scr., 52, 628
Butler K., 1984, PhD thesis, Univ. Lond., UK
Giddings J. R., 1981, PhD thesis, Univ. Lond., UK
Hauck B., Mermilliod M., 1998, A&AS, 129, 431
Huchra J., Willner S. P., 1973, PASP, 85, 85
Joshi S., Ryabchikova T., Kochukhov O., Sachkov M., Tiwari S. K., Chakradhari N. K., Piskunov N., 2010, MNRAS, 401, 1299
Kaiser A., 2006, in Aerts C., Sterken C., eds, ASP Conf. Ser. Vol. 349, Astrophysics of Variable Stars. Astron. Soc. Pac., San Francisco, p. 257
Kochukhov O. P., 2007, in Romanyuk I. I., Kudryavtsev D. O., Neizvestnaya O. M., Shapoval V. M., eds, Physics of Magnetic Stars. Nizhnij Arkhyz., p. 109
Kochukhov O., Tsymbal V., Ryabchikova T., Makaganyk V., Bagnulo S., 2006, A&A, 460, 831
Kochukhov O., Shulyak D., Ryabchikova T., 2009, A&A, 499, 851
Kupka F., Piskunov N., Ryabchikova T. A., Stempels H. C., Weiss W. W., 1999, A&AS, 138, 119
Kurucz R. L., 1992, in Barbuy B., Renzini A., eds, Proc. IAU Symp. 149, The Stellar Populations of Galaxies. Kluwer, Dordrecht, p. 225
Kurucz R. L., 1993, Kurucz CD-ROM 13. SAO, Cambridge
Kurucz R. L., Peytremann E., 1975, SAO Special Report, Vol. 362
LeBlanc F., Monin D., Hui-Bon-Hoa A., Hauschildt P. H., 2009, A&A, 495, 937
Lincke R., Ziegenbein G., 1971, Z. Phys. A, 241, 369
Matheron P., Escarguel A., Redon R., Lesage A., Richou J., 2001, J. Quantitative Spectrosc. Radiative Transfer, 69, 535
Michaud G., 1970, ApJ, 160, 641
Paunzen E., Stütz C., Maitzen H. M., 2005, A&A, 441, 631
Piskunov N. E., Kupka F., Ryabchikova T. A., Weiss W. W., Jeffery C. S., 1995, A&AS, 112, 525
Przybilla N., Butler K., Becker S. R., Kudritzki R. P., 2001, A&A, 369, 1009
Rufener F., 1976, A&AS, 26, 275
Rufener F., Nicolet B., 1988, A&A, 206, 357
Ryabchikova T., 2008, Contr. Astron. Obser. Skalnaté Pleso, 38, 257

Ryabchikova T., Piskunov N., Kochukhov O., Tsymbal V., Mittermayer P., Weiss W. W., 2002, A&A, 384, 545

Ryabchikova T., Leone F., Kochukhov O., 2005, A&A, 438, 973

Ryabchikova T., Ryabtsev A., Kochukhov O., Bagnulo S., 2006, A&A, 456, 329

Ryabchikova T., Fossati L., Shulyak D., 2009, A&A, 506, 203

Shulyak D., Tsymbal V., Ryabchikova T., Stütz Ch., Weiss W. W., 2004, A&A, 428, 993

Shulyak D., Ryabchikova T., Mashonkina L., Kochukhov O., 2009, A&A, 499, 879

Shulyak D., Ryabchikova T., Kildiyarova R., Kochukhov O., 2010, A&A, 520, A88

Skrutskie M. F. et al., 2006, AJ, 131, 1163

Smith G., Gallagher A., 1966, Phys. Rev., 145, 26

Tsymbal V. V., 1996, in Adelman S. J., Kupka F., Weiss W. W., eds, ASP Conf. Ser. Vol. 108, Model Atmospheres and Spectral Synthesis. Astron. Soc. Pac., San Francisco, p. 198

van der Bliek N. S., Manfroid J., Bouchet P., 1996, A&AS, 119, 547

van Leeuwen F., 2007, A&A, 474, 653

Wilke R., 2003, PhD thesis, Heinrich-Heine-Universität, Düsseldorf

This paper has been typeset from a TEX/LATEX file prepared by the author.